

The Case for SIMO Random Access in Multi-antenna Multi-hop Wireless Networks

Ahmed Khattab

Received: date / Accepted: date

Abstract In this paper, we demonstrate that multiple concurrent *asynchronous* and *uncoordinated* Single-Input Multiple-Output (SIMO) transmissions can successfully take place even though the respective receivers do not explicitly null out interfering signals. Hence, we propose simple modifications to the widely deployed IEEE 802.11 Medium Access Control (MAC) to enable multiple non-spatially-isolated SIMO sender-receiver pairs to share the medium. Namely, we propose to increase the physical carrier sense threshold, disable virtual carrier sensing, and enable message-in-message packet detection. We use experiments to show that while increasing the peak transmission rate, spatial multiplexing schemes such as those employed by the IEEE 802.11n are highly non-robust to asynchronous and uncoordinated interferers. In contrast, we show that the proposed multi-flow SIMO MAC scheme alleviates the severe unfairness resulting from uncoordinated transmissions in 802.11 multi-hop networks. We analytically compute the optimal carrier sense threshold based on different network performance objectives for a given node density and number of receive antennas.

Keywords Medium Access Control; Random Access; Fairness; Multiple-Input Multiple-Output (MIMO); Multi-hop 802.11 Networks.

1 Introduction

Random access Medium Access Control (MAC) protocols are susceptible to packet losses and unfairness in throughput distribution when the competing senders are not able to coordinate their transmissions. Increasing the underlying physical layer rate increases the rate of *only* MAC contention-winning flows. However, flows which are not able to win medium access still suffer very low throughput, despite their potentially high physical layer rate. It was experimentally shown using commodity hardware that an

Ahmed Khattab
The Center For Advanced Computer Studies (CACS)
University of Louisiana at Lafayette
Lafayette LA, 70504
Tel.: +1-713-884-0724
E-mail: akhattab@ieee.org

IEEE 802.11n flow can obtain a throughput of only a few hundred *k*bps in simple multi-hop topologies despite a few hundred *M*bps Multiple-Input Multiple-Output (MIMO) physical layer [20].

A key reason for the failure of the IEEE 802.11n to provide fairness is that the multi-antenna physical layer is used *only* to increase the per-link throughput (assuming fading and receiver noise are the only sources of randomness). However, such a physical layer does not counter *uncoordinated* or *hidden* senders, but instead relies on the 802.11 MAC to prevent their negative effects. In multi-hop random access networks, wherein senders are not necessarily within range, asynchronous interference from concurrent transmissions (i.e., interference not aligned to packet or frame boundaries) is unavoidable since nodes necessarily take uncoordinated transmission actions (e.g., starting time, power, or rate, etc.). Such interference cannot be explicitly canceled by the receiver because of the unavailability of the channel information of the asynchronous interferers. Recall that the preamble of an asynchronous interferer is non-decodable once the receiver is locked to its intended packet.

In this paper, we consider the additional source of randomness at the physical layer resulting from random and unpredictable interference from *uncoordinated* transmissions, and ask what is the best use of multiple antennas in this case. Unlike related information-theoretic [5, 7, 8, 14–16, 22, 32, 35, 36] and MIMO MAC [4, 6, 24, 29] approaches, we consider the uncoordinated interference scenario in asynchronous networks wherein a flow is unable to infer the interferers’ channels, rates, power selections, or starting times. We propose to have senders use only one transmit antenna and receivers use all of the available antennas. In such a Single-Input Multiple-Output (SIMO) strategy, the use of multiple receive antennas increases the diversity order or equivalently increases the received signal to interference plus noise ratio (SINR). The increase in the receive diversity allows the receiver to combat high interference levels and still retrieve packets with high reliability. Our use of SIMO decreases peak per-link rates compared to MIMO with spatial multiplexing, but increases the number of concurrent uncoordinated transmissions. Thus, our scheme is geared towards scenarios with problematic hidden and uncoordinated interferers. The contributions of the paper are as follows.

First, we experimentally¹ and analytically demonstrate that in the presence of uncoordinated interference, SIMO receive diversity provides increased robustness for a wide range of the signal to interference ratio (SIR) compared to MIMO spatial multiplexing schemes. Such schemes require significantly high SIR margin at the receiver to attain the promised gains. Thus, SIMO robust transmission is suitable when senders do not *a priori* know the SIR at the receivers. For example, using the WARP programmable open-access platform [19], we show that a 4×4 MIMO flow has to be more than 15 dB above an uncoordinated interferer to attain the $4 \times$ throughput gain. Meanwhile, a 1×4 SIMO flow’s transmission is almost error-free at -5 dB SIR. Furthermore, we show that for a given cumulative interference, SIMO reliability worsens with fewer uncoordinated interferers. Therefore, allowing more SIMO transmissions to take place at low transmission power is less harmful to the ongoing transmissions than allowing few high-power ones.

Second, we show how simple modifications to the IEEE 802.11n protocol can exploit the reliability of SIMO links to alleviate the consequences of uncoordinated transmissions. The main idea is to allow for *multiple* asynchronous spatially-proximate SIMO

¹ A preliminary set of our experiments was published in [18].

transmissions to take place rather than attempting to ensure that a single spatially-isolated flow uses MIMO to increase its rate (as the case with 802.11n). We show that this can be achieved by suitably increasing the physical carrier sense threshold and disabling virtual carrier sensing.² Consequently, a sender can initiate a new transmission – even if other nearby transmissions are currently taking place – as long as the cumulative interference in its vicinity implies a sufficient interference margin for an additional SIMO transmission. Meanwhile, a receiver must be able to lock on to a new arriving packet after receiving the preamble of an unintended packet. Thus, enabling the IEEE 802.11 Message-In-Message (MIM) [26] feature is mandatory for our multi-flow MAC approach. Simulation results show that our SIMO MAC alleviates the unfairness of legacy MIMO MAC in problematic topologies.

Finally, we analytically derive the SIMO MAC carrier sense threshold using a model in which uncoordinated interferers are uniformly distributed around a tagged node. Since a tagged receiver is unaware of the channel information of the interferers, we model the total interference as a single random variable. We show that the probability distribution of that random variable can be approximated by a gamma distribution, and provide closed form expressions of its statistics as a function of the node density and the number of receive antennas. We use this model to formulate the SIMO MAC sender’s transmission probability in order to compute the optimal carrier sense threshold achieving different network performance objectives.

The paper is organized as follows. We describe the system model and motivate the SIMO case in Section 2. In Section 3, we experimentally demonstrate SIMO robustness to uncoordinated interference. Then, we present simple modifications to the IEEE 802.11 to exploit SIMO flows to alleviate unfairness in Section 4. We analytically derive SIMO MAC carrier sense threshold for random networks in Section 5. We discuss related work in Section 6 and conclude in Section 7.

2 System Model and Motivation

In this section, we define the system model and the uncoordinated transmissions problems in random access networks. Then, we review the SIMO communications properties that entitle SIMO as the solution for such problems.

2.1 System Model

We consider a multi-hop ad-hoc network in which individual sender-receiver pairs may not be mutually within transmission range of each other. Each node is equipped with a half-duplex transceiver with $N > 1$ antennas tuned to the same frequency. All nodes in the network are competing for a common channel access according to an 802.11-like MAC based on Carrier Sense Multiple Access (CSMA). Competing senders independently decide whether or not to transmit based on the measured interference energy on the shared medium. The RTS/CTS collision avoidance mechanism is disabled to over-

² Virtual carrier sensing prohibits a node from transmitting after an overheard 802.11 packet header is decoded until after the packet’s duration field indicates that the transmission will be completed.

come the associated overhead.³ Nodes are not globally synchronized.⁴ Transmissions from out of range senders (*i*) asynchronously start at arbitrary time instants, and consequently, (*ii*) their channel information cannot be estimated by the receiver. Hence, multi-user detection or explicit interference cancellation techniques are not applicable. We refer to such out of range transmissions as *uncoordinated interference*. A receiver estimates the channel information of *only* its respective sender to retrieve the transmitted information using a maximal ratio combining architecture. Once a receiver locks to the preamble of its *intended* packet, it remains in the receive mode until the end of the packet reception. The impact of uncoordinated interfering transmissions at the physical layer is an increase in the ambient interference plus noise power.

2.2 Problem Definition and Motivation

Unlike scheduled access networks, the coordination of multiple asynchronous transmissions in random access networks is not feasible unless a separate resource is dedicated for coordination (e.g., a different channel, radio, or pilot tone). Consequently, random access protocols, such as 802.11, MACA, and MACAW, target having a single sender-receiver pair exclusively using all of the shared medium resources (e.g., time, bandwidth, and antennas, etc.) at a time barring spatial reuse. Other nearby senders must remain silent until the end of an ongoing transmission. In multi-hop networks, all nodes are not within range. Therefore, such random access MAC protocols yield uncoordinated interfering transmissions since nodes make independent and imperfect transmission decisions. The resulting collisions not only degrade the channel utilization but also lead to severe unfairness in the throughput received by competing sender-receiver pairs as shown in [11].

The 802.11n standard exploits a multi-antenna physical layer to realize high link rates via MIMO spatial multiplexing. However, the MAC layer still attempts to ensure a single spatially-isolated sender-receiver pair. In single-cell networks wherein all nodes are within range, the 802.11n MAC largely ensures such behavior. Consequently, in such idealized scenarios without hidden terminals, a transmission can utilize all of the MIMO channel's degrees of freedom (DoF: defined as the minimum of the link's transmit and receive antennas which is reflected by the rank of the channel matrix [31]) to increase its data rate via spatial multiplexing. Unfortunately, in multi-hop networks (or networks in which all nodes are *not* mutually within range yielding hidden nodes), the 802.11n MAC cannot ensure such interference-free condition due to the existence of uncoordinated senders.

Motivation. Our objective is to exploit the underlying multi-antenna physical layer to counter uncoordinated out of range interfering senders in 802.11 multi-hop networks. Instead of allowing only a single contention-winning flow per area to exclusively use MIMO to increase its rate, we ask what is the best multi-antenna scheme that allows multiple flows to simultaneously transmit. Unlike prior work [4, 6, 24, 29] which necessitates coordination among interfering flows, and hence requires network-wide synchronization, we consider uncoordinated random access system model in which

³ While RTS/CTS packet exchange can mitigate the effect of hidden terminals in some cases, it has no benefit in other cases and increases overhead in all cases [11].

⁴ Closed-loop MIMO schemes (e.g., beamforming, stream control, or optimal antenna selection) necessitate global node synchronization and information exchange overhead that outweighs the MIMO throughput gain [12].

senders independently take their transmission actions and receivers are unaware of the interference channel information.

2.3 SIMO Communications Background

Single-Input Multiple-Output (SIMO) communications utilize the multiple antennas at the receiver to provide diversity gain which translates into an increase of the wireless link reliability [30, 31]. It was shown that SIMO communications achieve lower error rates compared to open-loop transmit diversity schemes such as Alamouti [3] in the high SINR regime in both single-user and coordinated multi-user scenarios [31]. In addition to SIMO superior transmission reliability, Telatar’s conjuncture in the seminal paper [30] suggests using SIMO or few transmit antennas to maximize the outage capacity of the single-user non-ergodic channel. Recent studies have shown that SIMO communications asymptotically maximize the network capacity due to SIMO low outage probability and high transmission reliability [5, 8, 14–16, 32, 35]. It was also shown that an asymptotically high SINR margin is required at the receivers to obtain the multiplexing gain if multiple antennas are used for transmission. Such high SINR margin can be achieved in coordinated networks in which either a single spatially-isolated transmission is guaranteed or by jointly transmitting and decoding multiple transmissions which requires network-wide synchronization and induces significant overhead that outweighs the multi-antenna gain as was experimentally shown in [12].

In what follows, we generalize the case for SIMO communications raised by [5, 8, 14–16, 30, 32, 35] and consider asynchronous systems with uncoordinated transmissions. We use experiments to demonstrate the SIMO communications performance gains in the realistic setup in which (i) interfering transmissions can arbitrarily start during the course of a given transmission, and (ii) the intended receivers do not have any information whatsoever regarding interfering transmissions or the interference channel. It is worth mentioning that prior analytical results assume synchronized systems and/or assume the complete [5, 8, 14, 16, 32, 35] or the partial [16, 32] knowledge of the channel information of interfering transmissions. In Appendix A, we use outage analysis to prove the superior robustness of SIMO compared to MIMO spatial multiplexing if the receivers do not have the channel information of the interferers and simply employ single-user detection techniques.⁵ However, our analysis is limited to synchronized transmissions as the case with the related analytical work [5, 7, 8, 14–16, 22, 32, 35, 36].

3 Experimental Evaluation of SIMO Robustness to Uncoordinated Interference

In this section, we make the case for SIMO random access networks by experimentally demonstrating that (i) SIMO links provide increased robustness to uncoordinated (synchronous and asynchronous) interference as compared to MIMO links with spatial multiplexing for realistic channel conditions, (ii) the robustness of SIMO links degrades with fewer high-power interferers as compared to many low-power interferers with the

⁵ In this paper, we consider the simplest and widely deployed single-user architecture: the maximal ratio combiner without any information feedback to the sender. However, SIMO superiority has also been proven for more sophisticated architectures such as those addressed in [7, 8, 14–16, 22, 32, 36]. Section 6 presents a detailed discussion of such related work.

same cumulative interference power. Thus, enabling more SIMO flows to concurrently transmit (even at low-power since SIMO robustness depends on the SIR not the absolute transmission power) results in highly reliable links even with the receivers not explicitly handling the consequent uncoordinated interference. We analytically prove these properties (only for the aligned transmissions case) in Appendix A.

3.1 Testbed Setup

We use the Wireless Open-Access Research Platform (WARP) for our experiments [19]. WARP is an FPGA-based fully programmable wireless platform with four daughter card slots that can be used to implement up to 4x4 MIMO communication systems. We use the WARPLab framework which uses the WARP FPGA boards as wireless interfaces while the MIMO processing is performed by a PC to which up to 16 WARP boards can be connected via an Ethernet switch. Figure 1(a) depicts a schematic of an example 3-node WARPLab setup. The PC acts as a centralized controller which is used to (i) generate the transmitted data streams, (ii) realize the MAC scenarios under investigation (e.g., it controls which senders transmit, when, and with how many antennas), and (iii) post-process the received data streams. We implement a V-BLAST MIMO spatial multiplexing transceiver architecture [33]. We use maximal ratio combining to detect the transmitted signals.⁶ Each antenna is used for the transmission of an independent packet with a fixed power P . Thus, a $n \times N$ link implies n times the SIMO link transmission power. This transceiver automatically downscales to a SIMO one when only one antenna is used for transmission. The reported results are the average of five measurements.

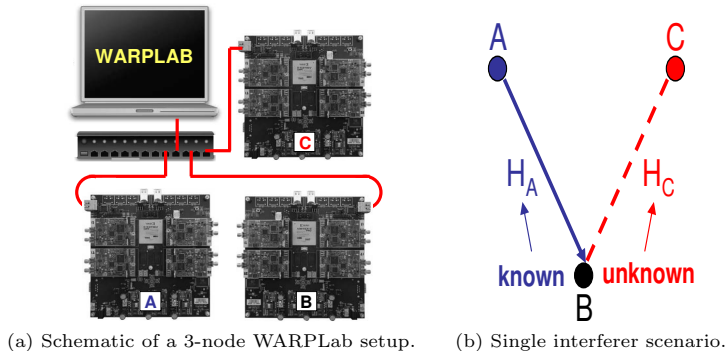


Fig. 1 A schematic of the 3-node baseline experiment.

Two precautions are made to ensure that any given MIMO link can utilize all of the available spatial DoF. First, the inter-spacing between the antennas connected to a WARP board is greater than twice the operating wavelength (we use 7 dBi omnidirectional external antennas operating at the 2.4 GHz ISM band). Second, the experiments

⁶ While non-linear detection and symbol cancellation techniques result in better performance for the V-BLAST architecture, the computational complexity of such optimal detectors is high. In this paper, we demonstrate SIMO transmission superiority with practical low-complexity detectors such as the maximal ratio combiners.

are performed in an indoor propagation environment characterized by rich scattering with none-line-of-sight paths between any sender and any receiver. For all experiments, individual link measurements indicated full rank channel matrices for all links. Therefore, all our findings are attributed to the interaction between the interfering transmissions rather than ill-conditioned links.

Scenario. Our experiments consider a single sender-receiver pair (WARP node A transmitting to WARP node B) with a different number of interfering nodes (WARP nodes C, D, \dots , etc.) depending on the tested scenario. Sender A as well as all the interferers are (i) at the same distance of 3.5 m from the receiver node B , and (ii) using the same MIMO schemes (i.e., the same number of transmit antennas) with respective transmit power per antenna P_A, P_C, \dots , etc. We independently tested the link from each sender to the common receiver (without interference) to ensure that all links obtain identical goodput for transmit power ranging between 0 dBm and 20 dBm. We define the relative SIR of the tagged sender A and an interferer I as the power ratio P_A/P_I , for $I = C, D, \dots$, etc. We also define the absolute SIR as the ratio of the power of the tagged sender A and the total interference power of all interfering senders, i.e., $P_A/\sum_I P_I$. For our experiment, P_A is set to 15 dBm and we vary the interferers' powers. Node B only estimates channel H_A and does not have the channel information of the interfering senders.

Tested MAC Approaches. We consider two MAC scenarios of the uncoordinated senders: (i) a random access MAC scenario in which the interfering senders are unaware of A 's ongoing transmission. Therefore, such interferers transmit during A 's packet transmission. This MAC scenario models hidden senders in 802.11n multi-hop networks. (ii) A perfect scheduler MAC scenario in which the PC allows only one sender to transmit at a time with equal channel access time guaranteed per sender. The perfect scheduler does not include coordination and information distribution overhead of an actual protocol and serves as a benchmark for comparison. The goodput of the perfect scheduler represents the upper bound of what can be achieved by a MAC protocol that allows competing flows to share the medium in TDMA manner.

3.2 Reliability of SIMO Links with Uncoordinated and Asynchronous Interference

In this experiment, we show that SIMO robustness to uncoordinated interference compared to MIMO spatial multiplexing holds for real systems *irrespective of the temporal alignment of the uncoordinated interference*. For the tagged link AB , we consider a single equidistant interfering node C . Figure 1(b) depicts the experiment scenario. We consider two cases for uncoordinated random access: A full- and mid-packet interference scenarios wherein C 's transmissions start exactly with and exactly in the middle of A 's transmissions, respectively. Figures 2 and 3 depict the goodput of link AB normalized to the interference-free SIMO goodput for the tested MAC approaches in 2- and 4-antenna systems for full- and mid-packet interference, respectively.

SIMO Robustness. As shown in both figures, $N \times N$ MIMO spatial multiplexing requires high SIR to achieve the $N \times$ goodput gain, regardless of the temporal alignment of the uncoordinated interference. For example, link AB needs to be more than 15 dB above the interferer to obtain the goodput gain for full-packet interference. In contrast, almost all of the packets of the $1 \times N$ SIMO transmissions are successfully received resulting in almost unity normalized rate even at low SIR values. The reliability of a SIMO link increases with the number of receive antennas due to the increase in the

available DoF. Thus, a 1×4 transmission achieves unity normalized goodput at -5 dB while a 1×2 requires at least 2.5 dB SIR.

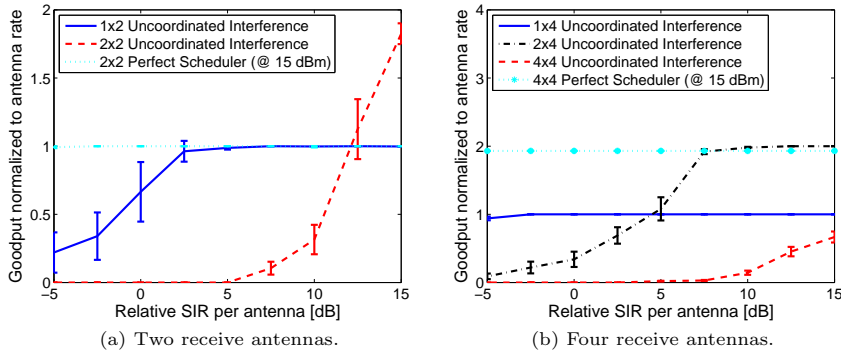


Fig. 2 Full-packet interference goodput of link AB versus the relative SIR. For the perfect scheduler, link AB is interference-free and $P_A = 15$ dBm.

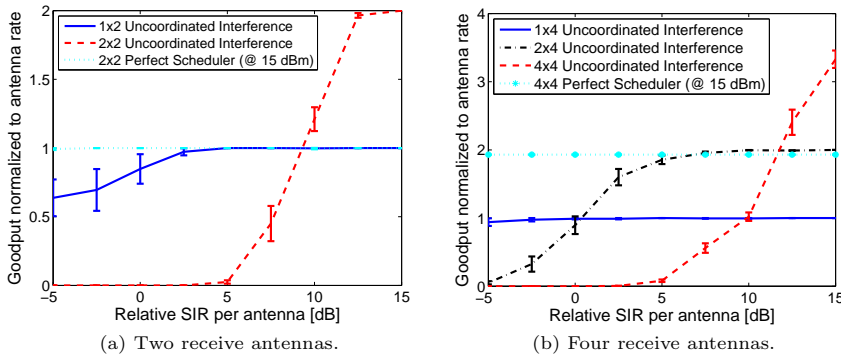


Fig. 3 Mid-packet interference goodput of link AB versus the relative SIR. For the perfect scheduler, link AB is interference-free and $P_A = 15$ dBm.

Note that the goodput of the 1×4 link AB is only 55% of its upper bound. The perfect scheduler goodput bound can still be attained in the presence of C 's interference if A and C use two antennas each. Yet, A must be at least 5 dB stronger than C . Therefore, an optimal MAC must track the SIR at the receiver side in order to choose the optimal spatial multiplexing degree. However, such coordination (i) induces overhead which further degrades the goodput, (ii) does not guarantee optimality as the SIR can change during the course of a packet transmission due to the asynchronicity of uncoordinated transmissions. Interested readers are referred to [20] for further discussion of SINR-based selection of the spatial multiplexing degree. In Section 4, we show that 1×4 SIMO will allow more flows to be simultaneously active as the node density increases, and hence, leads to higher network goodput compared to 1×2 SIMO.

Temporal Alignment of Interference. Next, we investigate the impact of the interference temporal alignment. For a given goodput, the SIR required given mid-packet interference is lower as compared to full-packet interference – despite similar general trends. This is attributed to two reasons. First, receiver B is receiving A 's preamble in the absence of interference from C when C starts in the middle of A 's packet transmission. Hence, B has a more accurate estimate of H_A compared to the full-packet interference case wherein A 's preamble is interfered by C 's transmission. Second, only half of A 's payload bytes are susceptible to interference from C . The percentage of successfully received packets increases with the decrease in the overlap time between the two transmissions. We do not further investigate this issue. Note that, all our findings apply to TDMA scheduled access systems given the full-packet interference results. However, scheduled access is beyond the scope of this paper.

3.3 Multiple SIMO Transmissions Scenarios

In this experiment, we investigate the impact of the number of interferers in multi-interferer scenarios. The total interference power is fixed and we vary the number of interferers that generates such cumulative interference.⁷ Our evaluation metric is the packet delivery ratio defined as the percentage of packets that are successfully received out of the total number of transmitted packets. We plot the packet delivery ratio of the tagged link AB given a fixed cumulative interference power while varying the number of interferers for a 2-antenna receiver in Figure 4. All senders (including A) are at the same distance from the receiver B . All interferers start at the same time. The x-axis represents the absolute SIR (defined as the ratio of sender A 's power and the sum of the power of all interferers). We split the cumulative power equally among all interferers.

Figure 4 shows that the effect of uncoordinated interference is weakened as the number of the interferers increases for a fixed cumulative interference. This behavior is illustrated with the increase in the packet delivery ratio as the number of interferers increases. This is attributed to the fact that the assumed single-user detection treats the cumulative interference as a single source of randomness, and does not have any information to null out individual interferers. The complex-valued signals transmitted from different interferers undergo different complex-valued channels. The cumulative interference vector is the phasor addition of the received interference vectors. Due to the randomness in the phases of the received signals from different interferers, their phasor addition yields cumulative interference of amplitude much less than the sum of the amplitudes of the individual received interference vectors. In other words, multiple weak interferers will have the same effect of a single interferer with same total power only if their received vectors are in phase (which is true with probability zero).

Figure 5 depicts the transmitted and the received (at the matched filter output) symbol constellations of 10 packets for 1 and 4 interferers at 0 dB absolute SIR for the 2-antenna system. The variance of the received symbols decreases with the increase of the number of interferers due to the reduction of interference effect given multiple

⁷ We also studied the case in which we vary the total cumulative interference power by varying the number of interferers while fixing the transmission power per interferer. We found that 70-83% of the packets of a $1 \times N$ are successfully received in the presence of $N - 1$ interferers each with the same transmit power as the tagged sender. In theory [31], a 100% transmission success ratio can be achieved if and only if the channel information of all interferers is known which is infeasible in asynchronous networks.

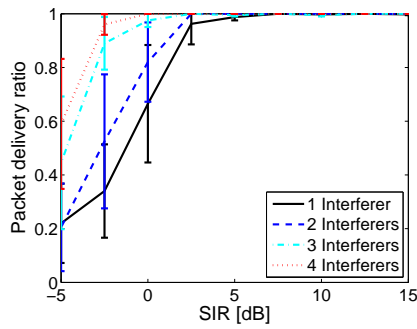


Fig. 4 Goodput of link AB versus the absolute SIR.

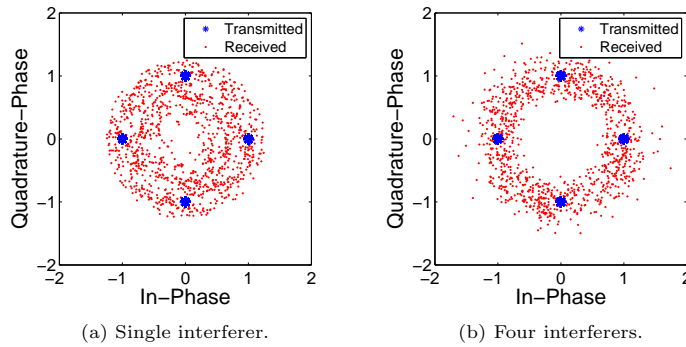


Fig. 5 Transmitted and received symbol constellations at the matched filter output for 0 dB SIR.

interferers. This implies that a few strong uncoordinated interferers are more harmful to an ongoing transmission compared to many weak interferers. Similar performance was attained in the 4-antenna system. Furthermore, we repeated this experiment for a SISO system and observed a similar trend. It is worth mentioning that our experimental results provide a rigorous explanation of prior analytical results that showed similar weakening of the interference effect with the increase of the number of interferers for a given total interference power [34]. We further generalize such results by considering more interferers to validate this point in a realistic propagation environment.

3.4 Summary of the Results

We conclude this section by highlighting the main two results of our experiments. These two results form the basis upon which our non-greedy multi-flow SIMO random access approach is built in the next section.

- MAC protocols exploiting MIMO to increase the per-link rate cannot obtain the spatial multiplexing gain in the presence of a significant uncoordinated transmission. On the other hand, SIMO reliable transmission is resilient to uncoordinated interference without explicit interference suppression and irrespective of the temporal alignment of the interference.

- The robustness of a SIMO link worsens in the presence of few high-power interferers compared to many low-power ones with equivalent cumulative interference power. The impact of many weak interferers resembles the noise effect. Thus, a non-greedy MAC should allow multiple SIMO transmissions to occur instead of allowing a single transmission to greedily capture all of the channel resources in multi-hop networks with uncoordinated sender-receiver pairs.

4 SIMO Fair Random Access MAC

In this Section, we present the physical and MAC layer modifications required to allow multiple non-spatially-isolated SIMO flows to successfully communicate and demonstrate the gains compared to legacy MIMO MAC.

4.1 802.11n Physical and MAC Layer Modifications

Our multi-flow SIMO MAC scheme relies on the ability of sender-receiver pairs to initiate new transmissions – if possible – even if proximate sender-receiver pairs are active. However, the 802.11 standard and its multi-antenna version (the 802.11n) target having a single transmission per unit area. We show that only two modifications are required to 802.11n physical and MAC layers to enable multi-flow SIMO communications. Namely, *(i)* preventing a single sender-receiver pair from exclusively reserving the medium by suitably increasing the physical carrier sense threshold and disabling virtual carrier sensing, and *(ii)* modifying the packet detection at the physical layer to track the relative changes in the Received Signal Strength Indicator (RSSI) value to allow receivers to lock to new packets in the presence of active transmissions.

4.1.1 Exclusive Medium Reservation Prevention

According to the 802.11 MAC, a sender decides whether or not to transmit based on physical and virtual carrier sensing. If the physical carrier sensing implies that the cumulative energy on the medium exceeds a certain threshold over a DIFS period, a sender infers the existence of a nearby transmission. In order to not cause the ongoing transmission to collapse, legacy physical carrier sense threshold is chosen to allow a single transmission per carrier sensing area. In contrast, we propose to suitably increase the carrier sense threshold in order to allow for multiple transmissions to coexist per carrier sensing area. Therefore, a sender can still transmit - even if other nearby transmissions are currently taking place - as long as the cumulative interference is below the new threshold. In Section 5, we compute the optimal carrier sense threshold for a given node density.

Recall that our approach allows for multiple *asynchronous* transmissions to take place. A sender does not have to wait for a particular ongoing transmission to end. Instead, a sender must continually perform physical carrier sensing in order to initiate its transmission once the cumulative interference implies non-saturated medium. Therefore, virtual carrier sensing must be disabled for proper operation.

4.1.2 Message-In-Message (MIM) Packet Detection

In order for multiple asynchronous flows to successfully take place, the receivers of different flows must be able to lock to the preamble of a new packet if the current active transmissions are not of interest (i.e., not intended to this particular receiver). This can be easily achieved by monitoring the RSSI changes after receiving the preamble of an unintended packet. If the relative change in RSSI exceeds a certain threshold, a receiver infers the existence of a new packet and locks on to the new preamble. This functionality can be easily implemented by enabling the 802.11 optional Message-In-Message (MIM) feature [26]. MIM is an enhancement to 802.11 physical layer to address physical layer capture by locking to a new arriving stronger packet. However, MIM is not implemented in all 802.11 chipsets as it is not mandated by the standard. For our multi-flow MAC approach, the MIM feature (or similar packet detection mechanism) is mandatory.

4.2 Performance Evaluation

Here, we demonstrate the performance gains obtained via the above simple physical and MAC layer modifications. We study the fairness and the goodput achieved by the modified 802.11 on top of a SIMO physical layer compared to legacy 802.11 running on top of a MIMO $N \times N$ spatial multiplexing physical layer. Our fairness index is the sum of the log utility which is maximized via the proportionally fair flow rates [17]. We developed a custom event driven simulator using MATLAB. We extract the physical layer parameters of the WARPLab platform and use our experimental data to build a lookup table that is used by the simulator to learn the physical layer behavior. For both the SIMO and MIMO MAC realizations, we use DIFS, SIFS, and mini-slot durations of 36, 20, and 20 μ s, respectively. Binary exponential backoff is used for contention windows in the range [31, 1023]. The maximum retry limit is 7 attempts before a packet is discarded. In all the considered topologies, senders A and B are out of each other's carrier sensing range for both the SIMO and MIMO systems.

Information Asymmetry Topology. According to legacy MIMO 802.11, flow Aa receives significantly low goodput compared to flow Bb in the information asymmetry topology depicted in Figure 6(a). While both senders are unable to coordinate their transmissions, only A 's packets collide at its intended receiver a while B 's packets are successfully received at b . Thus, only flow Aa suffers high packet loss and backoff penalties. Normalizing the goodput of each flow by that of a single $N \times N$ flow, the total log utility is -1.19 and -1.22 for the 2- and 4-antenna systems, respectively. The proportionally fair maximum log utility is -0.6 achieved when both flows obtain half of the $N \times N$ flow rate. In contrast, the proposed SIMO MAC approach allows a to successfully receive most of its intended packets despite B 's uncoordinated transmissions. Thus, the goodput of flow Aa increases, and hence, the total log utility increases to -0.84 and -1.14 for the 2- and 4-antenna systems, respectively. While SIMO MAC log utility is close to optimal in the 2-antenna case, the log utility degradation is due to SIMO low per-flow goodput in the 4-antenna system.

Flow in the Middle Topology. In the topology depicted in Figure 6(b), the senders of the two outer flows Aa and Bb are out of each other's range. Thus, both flows independently and successfully transmit to their respective receivers. According to 802.11 MIMO MAC, the sender of the middle flow is deferring as long as either or

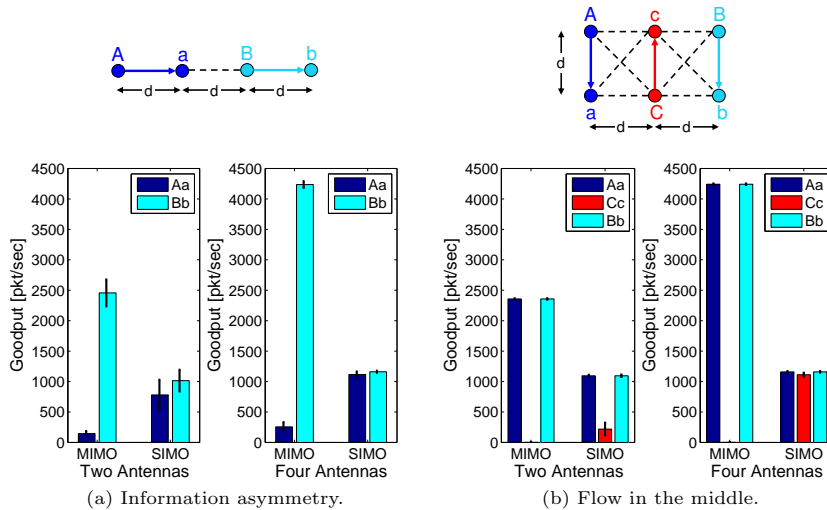


Fig. 6 Example problematic multi-hop topologies with uncoordinated transmissions. Solid arrows indicate data flows while dashed lines imply nodes are within transmission range. Senders A and B are uncoordinated (out of range).

both the outer flows are active and receives almost zero goodput. The total log utility for the 2- and 4- antenna systems is -4.67 and -4.62 , respectively; which is much lower than the proportionally fair utility of -0.83 achieved by a goodput of 0.67 , 0.33 , and 0.67 . In contrast, the proposed SIMO approach allows the middle flow to transmit despite the ongoing activities of the outer flows. In the 4- and 2-antenna systems, the achieved goodput is $(0.27, 0.26, 0.27)$ and $(0.46, 0.09, 0.46)$, yielding log utilities of -1.7 and -1.69 , respectively. In the 2-antenna system, the degradation in the goodput of the middle flow is because such flow is receiving interference from two strong interferer. Recall that the performance of our SIMO approach is significantly dependent on the instantaneous interference unlike legacy 802.11 which targets a binary on-off interference model. For example, if the inter-flow distance slightly increases to $1.2d$ while keeping the sender-receiver distance at d , the log utility increases to -1.2 as the achieved rates increase to 0.5 , 0.21 , and 0.5 due to reduced interference.

Hidden Senders Scenarios. Finally, we consider uncoordinated senders scenarios wherein long-term fairness is not the main concern (i.e., all flows operate under identical interference conditions). We consider 2- and 4-flow scenarios wherein all senders are hidden from each other and all senders are at the same distance from the collocated receivers. Both the SIMO MAC and MIMO MAC approaches yield almost equal throughput per flow as depicted in Figures 7(a) and (b). However, SIMO MAC results in less collisions, and hence, better short-term fairness as indicated by the variance of the goodput depicted via the error bars. In the 2-flow topology depicted in Figure 7(a), the goodput achieved by the SIMO MAC is less than the MIMO MAC in the 4-antenna case due to SIMO low per-flow rate. However, as the number of competing flows increase, the number of simultaneously active flows increase with the number of antennas, and the SIMO average flow rate approaches the MIMO flow rate (both almost equal to 0.2). Even for the 2-antenna system, the per flow goodput in the 4 flow topology (0.17) is close to the MIMO case (0.19). In the next section, we analytically

study the relationship between the node density (hence, the number of interferers), N , and the per flow achievable rate in random network topologies.

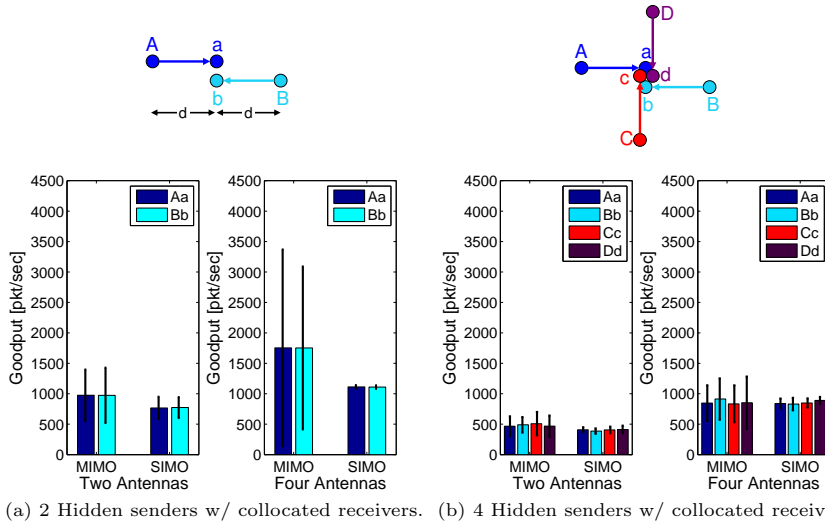


Fig. 7 Example hidden terminal topologies. Senders A and B are uncoordinated (out of range) senders in topology (a). All senders in topology (b) are out of range. Receivers are collocated.

5 SIMO Carrier Sense Threshold for Random Networks

In this section, we compute the SIMO MAC carrier sense threshold. First, we find the distribution of the cumulative interference power at an arbitrary node. Using this distribution, we formulate the node's transmission probability in terms of the carrier sense threshold. For a given network performance objective, the SIMO MAC carrier sense threshold is computed by reversing the node's transmission probability that achieves the targeted objective.

5.1 System Model

We consider single-hop flows in a multi-hop wireless network in which nodes are uniformly distributed within an area. We ignore the edge effects and assume that all links have the same statistical characteristics. Each node is equipped with $N \geq 1$ antennas. A node always uses all N antennas in the receive mode (e.g., for packet reception or RSSI measurement). Meanwhile, a sender uses one antenna for transmission. The transmit power P is uniform throughout the network.

Consider a specific node, we denote the number of interfering transmissions resulting in co-channel interference at a given time instant as L . The number of interferes L is a random variable that depends on the node density ρ . We assume uniform backlogged traffic at all senders. Since the neighborhood observed by each node in an arbitrary

topology is statistically identical, the L interferers can be assumed to be uniformly distributed within a disc of radius D centered at the tagged receiver, where D is the largest distance at which an interfering transmitter can cause interference above the receiver sensitivity at the tagged receiver. Recall that we have demonstrated that the impact of multiple weak interferers resembles noise. Thus, we only consider strong interferers within D . Let ϵ denote an infinitesimal distance such that it does not affect the uniform distribution of nodes. The probability density function of the distance between a node and the tagged receiver is given by

$$f_D(d) = \frac{2d}{D^2 - \epsilon^2}, \quad d \in [\epsilon, D] \quad (1)$$

5.2 Cumulative Interference Distribution

For the aforementioned system model, the received power from the k^{th} interferer is given by

$$P_k = P_0 \left(\frac{d_0}{d_k} \right)^\alpha \gamma_k \quad (2)$$

where d_k is the distance between the k^{th} interferer and the tagged node, d_0 is the close-in reference distance, P_0 is the received power at the close-in reference distance, α is the path loss exponent of the environment, and γ_k is the effective channel fading parameter between the antenna of the k^{th} interferer and the N antennas of the tagged node. For Rayleigh fading channels, γ_k follows a Chi-square distribution with $2N$ degrees of freedom [1, 10, 31], i.e.,

$$f_{\chi^2}(\gamma) = \frac{1}{\Gamma(N)} \gamma^{N-1} e^{-\gamma} \quad (3)$$

The cumulative received interference power at the tagged node, P_{rssi} is the sum of the L *i.i.d.* random variables P_k , i.e.,

$$P_{rssi} = P_1 + P_2 + \dots + P_L \quad (4)$$

Note that the random variable L is independent of the random variables P_k . In a highly dense network, the number of active senders in the network follows a Poisson distribution. The probability of having l active senders in the network is given by

$$Prob[L = l] = \frac{L_0^l e^{-L_0}}{l!} \quad (5)$$

where $L_0 = \pi R^2 \rho$ is the average number of interfering nodes, where ρ is the node density of the network. Using the law of total probability, the probability distribution function of P_{rssi} can be calculated as follows

$$Prob[P_{rssi}] = \sum_{l=0}^{\infty} Prob[P_{rssi} \setminus L = l] Prob[L = l] \quad (6)$$

The conditional distribution of P_{rssi} is difficult to obtain in closed form. Meanwhile, the characteristic function of P_{rssi} conditioning on $L = l$ is simply $(\phi_{P_k}(w))^l$, where $\phi_{P_k}(w)$ is the characteristic function of the *i.i.d.* random variables P_k . Using the law to

total probability, the unconditional characteristic function of P_{rssi} , $\phi_{P_{rssi}}(\omega)$, is given by

$$\phi_{P_{rssi}}(\omega) = \sum_{l=0}^{\infty} (\phi_{P_k}(\omega))^l \frac{L_0^l e^{-L_0}}{l!} \quad (7)$$

$$= e^{L_0(\phi_{P_k}(\omega)-1)} \quad (8)$$

In order to compute $\phi_{P_k}(\omega)$, we first compute the characteristic function of the received power of the k^{th} interfering node conditioning on a channel fading instance $\phi_{P_k|\gamma}(w) = \mathbb{E}[e^{jwP_k} | \gamma_k = \gamma]$, then we integrate over the distribution of the channel fading distribution to obtain the characteristic function $\phi_{P_k}(w)$ of the random variable P_k . We obtain (the detailed proof is in Appendix B)

$$\phi_{P_k}(w) = \frac{2P_0^{2/\alpha} d_0^2}{\alpha(D^2 - \varepsilon^2)} \int_{(\frac{d_0}{D})^\alpha P_0}^{(\frac{d_0}{\varepsilon})^\alpha P_0} \frac{1}{x^\beta (1 - j\omega x)^N} dx \quad (9)$$

$$= Cf(\beta, N, \omega) \quad (10)$$

where the variables C and β represent the constants $\frac{2P_0^{2/\alpha} d_0^2}{\alpha(D^2 - \varepsilon^2)}$ and $(\alpha + 2)/\alpha$, respectively, for the ease of notation.

Given $\phi_{P_k}(\omega)$ in (9), it is difficult to reverse $\phi_{P_{rssi}}(\omega)$ to obtain the distribution of P_{rssi} . Recall that P_{rssi} is the sum of small positive numbers. Therefore, the distribution of P_{rssi} can be modeled using a Gamma distribution according to the central limit theory for casual functions [23]. Using $\phi_{P_k}(\omega)$ to obtain the mean and variance of P_{rssi} , the probability distribution of P_{rssi} is given by

$$f_{P_{rssi}}(y) = y^{a-1} \frac{e^{-y/b}}{b^a \Gamma(a)}, \quad y > 0 \quad (11)$$

where $a = \mathbb{E}^2(P_{rssi})/Var(P_{rssi})$ and $b = Var(P_{rssi})/\mathbb{E}(P_{rssi})$. $\mathbb{E}(P_{rssi})$ and $Var(P_{rssi})$ are evaluated using the first and second moments of $\phi_{P_{rssi}}(\omega)$ calculated as

$$\begin{aligned} \mathbb{E}(P_{rssi}) &= -j\dot{\phi}_{P_{rssi}}(0) \\ &= CL_0 \dot{f}(\beta, N, 0) e^{L_0(Cf(\beta, N, 0)-1)} \end{aligned} \quad (12)$$

and

$$\begin{aligned} \mathbb{E}(P_{rssi}^2) &= -\ddot{\phi}_{P_{rssi}}(0) \\ &= CL_0 [\dot{f}(\beta, N, 0) + CL_0 \dot{f}^2(\beta, N, 0)] e^{L_0(Cf(\beta, N, 0)-1)} \end{aligned} \quad (13)$$

Using the properties of the beta functions, $f(\beta, N, 0)$, $\dot{f}(\beta, N, 0)$, and $\ddot{f}(\beta, N, 0)$ can be computed as

$$f(\beta, N, 0) = -\frac{((\frac{d_0}{D})^\alpha P_0)^{1-\beta} - ((\frac{d_0}{\varepsilon})^\alpha P_0)^{1-\beta}}{1-\beta} \quad (14)$$

$$\dot{f}(\beta, N, 0) = -jN \frac{((\frac{d_0}{D})^\alpha P_0)^{2-\beta} - ((\frac{d_0}{\varepsilon})^\alpha P_0)^{2-\beta}}{2-\beta}, \alpha \neq 2 \quad (15)$$

$$\ddot{f}(\beta, N, 0) = N(N+1) \frac{((\frac{d_0}{D})^\alpha P_0)^{3-\beta} - ((\frac{d_0}{\varepsilon})^\alpha P_0)^{3-\beta}}{3-\beta} \quad (16)$$

Model Validation. Next, we validate the accuracy of modeling the distribution of P_{rssi} by a gamma distribution and show that our analysis closely captures the parameters of the distribution. We assume time is slotted. In each slot, we choose the number of interfering senders from a Poisson distribution with parameter L_0 . Figures 8 and 9 depict the empirically and analytically computed distribution of P_{rssi} for $L_0 = 4$, and its statistics for different values of L_0 , respectively.

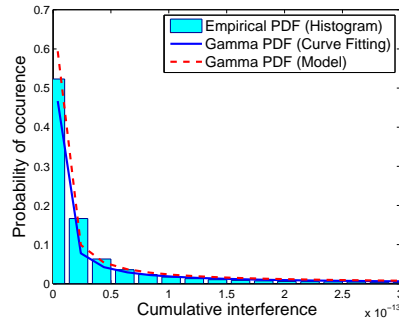


Fig. 8 Model validation of the P_{rssi} distribution. $P_0 = 0.44$ mW, $D = 250$ m, $d_0 = \epsilon = 12.5$ cm, $\alpha = 4$, $N = 4$ antennas, and $L_0 = 4$ interferers.

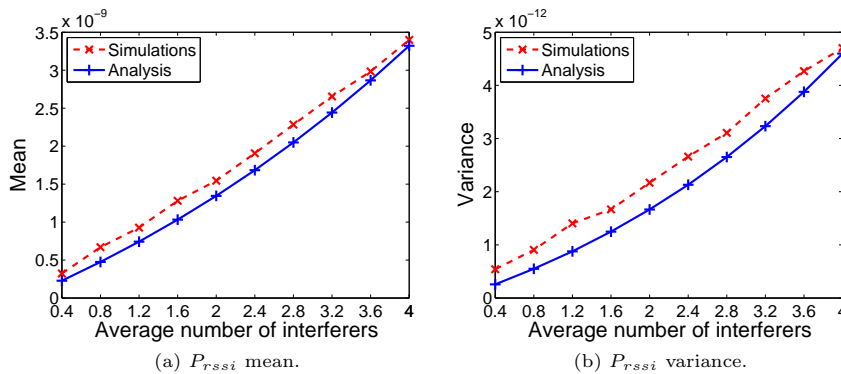


Fig. 9 The analytically computed statistics of P_{rssi} closely matches the empirical ones for wide range of interfering transmissions.

Node's Transmission Opportunity. Given the cumulative interference distribution $f_{P_{rssi}}(y)$ in (11), a node's transmission probability p_{tr} is computed by integrating $f_{P_{rssi}}(y)$ up to the carrier sense threshold CS_{th} . Recall that SIMO MAC permits a sender to transmit only if the cumulative interference is below CS_{th} . Furthermore, the value of CS_{th} for the proposed SIMO MAC is different from the carrier sense threshold of legacy 802.11n MIMO MAC due to the SIMO MAC modifications discussed in Section 4. In what follows we show to compute SIMO MAC carrier sense threshold.

5.3 SIMO MAC Carrier Sense Threshold

Here, we compute the SIMO MAC carrier sense threshold CS_{th} that achieves certain network performance objectives. In order to do so, we need to define the SIMO MAC achievable rate per unit area of the network. Due to the independence of the interference at a flow's endpoints, the achievable rate per unit area is

$$R = r(1 - p_{out})p_{tr}\rho \quad (17)$$

where p_{out} is the outage probability of a given transmission defined as the probability of the event that the mutual information $I(SINR) = \log_2(1 + SINR)$ falls below a specific transmission rate r [31], i.e.,

$$p_{out} = Prob[I(SINR) < r]. \quad (18)$$

One way to compute CS_{th} is to assume an outage-constrained network in which a small outage (typically $p_{out} < 0.1$) is targeted to guarantee a certain service requirement. For the targeted p_{out} , the optimal contention density $\bar{\rho}$, defined as the number of successful transmissions per unit area, can be computed by manipulating the results in [15] and [32] derived for closed-loop MIMO systems with maximal ratio transmission. The computed optimal contention density $\bar{\rho}$ translates to the transmission capacity of the network defined in [14–16, 32] as $r(1 - p_{out})\bar{\rho}$. Substituting in (17) with the assumed p_{out} and equating R with the calculated transmission capacity, we numerically compute the carrier sense threshold of the SIMO MAC protocol that achieves the network transmission capacity using the gamma incomplete function.

Alternatively, we can compute CS_{th} that yields a service requirement defined in terms of a targeted rate per unit area. This can be achieved by directly computing p_{out} as a function of the network parameter using the cumulative interference distribution then substituting in (17). The maximal ratio combiner uses the channel gain vector of the tagged sender as the weight vector to be multiplied by the received signal [1, 10]. Hence, the SINR at the output of the receiver's maximal ratio combiner is given by

$$SINR = \frac{\tilde{P}_s \mathbf{h}_s^\dagger \mathbf{h}_s}{\sum_{k=1}^L \tilde{P}_k \frac{|\mathbf{h}_s^\dagger \mathbf{h}_k|^2}{\mathbf{h}_s^\dagger \mathbf{h}_s} + \sigma^2} \quad (19)$$

where $\tilde{P}_s = P_0(\frac{d_0}{d_s})^\alpha$ and $\tilde{P}_k = P_0(\frac{d_0}{d_k})^\alpha$ are the path-loss component of the received signal power from the tagged sender s and the k^{th} interferer given in (2), respectively; \mathbf{h}_s and \mathbf{h}_k are the vector channel gains of the tagged sender and the k^{th} interferer, respectively, and \dagger is the complex conjugate transpose. We assume additive white Gaussian noise at the receiver with variance σ^2 . For the ease of notation, we denote $\gamma = \mathbf{h}_s^\dagger \mathbf{h}_s$ and $\tilde{\gamma} = \sum_{k=1}^L \tilde{P}_k \frac{|\mathbf{h}_s^\dagger \mathbf{h}_k|^2}{\mathbf{h}_s^\dagger \mathbf{h}_s}$. For the assumed Rayleigh fading environment, the elements of \mathbf{h}_s and \mathbf{h}_k follow a complex Gaussian distribution with zero mean and unit variance. Hence, γ follows the Chi-square distribution given in (3) with $2N$ degrees of freedom. According to [1, 10], $\frac{|\mathbf{h}_s^\dagger \mathbf{h}_k|^2}{\mathbf{h}_s^\dagger \mathbf{h}_s}$ follows an exponential distribution. Using a similar analysis as in Section 5.2, we find that $\tilde{\gamma}$ follows the Gamma distribution given by (11) with the parameters in (12) to (16) computed using $N = 1$. Substituting with (19) in (18), the outage probability can be expressed as

$$p_{out} = Prob\left[\frac{\tilde{P}_s \gamma}{\tilde{\gamma} + \sigma^2} < (2^r - 1)\right] \quad (20)$$

Using the distributions of γ and $\tilde{\gamma}$ given by (3) and (11), respectively, the outage probability in (20) is calculated as

$$p_{out} = \int_0^\infty f_{\tilde{\gamma}}(\tilde{\gamma}) \int_0^{A(\tilde{\gamma}+\sigma^2)/\tilde{P}_s} f_\gamma(\gamma) d\gamma d\tilde{\gamma} \quad (21)$$

$$= 1 - \frac{e^{-\frac{A\sigma^2}{\tilde{P}_s}}}{b^a \Gamma(a)} \sum_{s=0}^{N-1} \frac{(A/\tilde{P}_s)^s}{s!} \int_0^\infty \tilde{\gamma}^{a-1} (\tilde{\gamma}+\sigma^2)^s e^{-\tilde{\gamma}(\frac{1}{b}+\frac{A}{\tilde{P}_s})} d\tilde{\gamma} \quad (22)$$

where $A = (2^r - 1)$. In interference-limited networks, where both the received signal power and the interference power are much higher than the noise power (i.e., $\tilde{P}_s \gg \sigma^2$ and $\tilde{\gamma} \gg \sigma^2$), the intractable integral in (22) is reduced to a tractable one that equals to $\Gamma(a+s) \left(\frac{b\tilde{P}_s}{\tilde{P}_s+Ab}\right)^{s+a}$. Hence, the outage probability in interference-limited scenarios is calculated as

$$p_{out} \cong 1 - \frac{1}{(1+Ab/\tilde{P}_s)^a} \sum_{s=0}^{N-1} \frac{\Gamma(a+s)}{s! \Gamma(a)} \left(\frac{Ab/\tilde{P}_s}{1+Ab/\tilde{P}_s}\right)^s \quad (23)$$

Note that, the outage probability, and hence, the achievable flow rate rate are functions of the transmission rate r , the number of receive antennas N , the transmit power P , and the node density ρ reflected by a and b . For a targeted rate per unit area, the only unknown in (17) is the SIMO MAC carrier sense threshold which is numerically computed using the gamma incomplete function.

6 Related Work

The related literature of MIMO networks and unfairness mitigation in random access networks can be summarized as follows.

MIMO-specific MAC. The upcoming IEEE 802.11n MIMO standard promises high throughput via MIMO spatial multiplexing. However, because the MIMO physical layer does not consider uncoordinated interference, the 802.11n suffers from the same severe unfairness and starvation problems encountered in single antenna networks [20]. In contrast to the IEEE 802.11 standards, multiple simultaneous transmissions can coexist in the same channel using joint MIMO signaling techniques such as stream control, beamforming, or optimal antenna selection. However, protocols employing these mechanisms, such as [4, 6, 24, 29], require network-wide synchronization and channel information of all interfering transmitters at each receiver (and/or senders) in order to null out their signals. While such synchronous MAC protocols address fairness by allowing multiple simultaneous transmissions, the overhead due to network synchronization and channel acquisition significantly degrades the system throughput as was empirically shown in [12]. The only related work that addressed MIMO multiple transmissions in asynchronous networks is [20]. In [20], the MIMO spatial multiplexing degree was probabilistically determined based on the SINR at the receiver. However, such scheme cannot be incrementally deployed to the widely used 802.11 as the case with SIMO MAC and necessitates per-transmission sender-receiver coordination.

Alternative Random MAC Approaches. Due to the inefficiency and unfairness problems of random access in single radio multi-hop networks, several alternative

approaches have been proposed in the literature. Examples include the use of multiple orthogonal channels [28] and/or multiple radios [2], and the use of directional antennas [9]. Even though such alternatives have the potential of addressing the hidden terminals problem and its consequences, additional resources are required to realize interference-free parallel transmission. Furthermore, such solutions introduce new medium access challenges such as coordination and deafness problems. Alternatively, [13] and [25] present new physical layer designs, such as joint decoding of collided packets and self interference cancellation, respectively, to counter the effects of hidden terminals. In contrast, we address random access inefficiencies via simple MAC modifications in single-channel multi-hop networks with conventional multi-antenna physical layer.

Performance Analysis of MIMO ad-hoc Networks. With the proliferation of the MIMO technology, recent works have been concerned with characterizing the capacity of MIMO ad-hoc networks [5, 7, 8, 14–16, 22, 32, 35, 36] rather than the performance of an individual MIMO link. In [5] and [35], the optimal signaling scheme of interfering MIMO transmissions have been *asymptotically* studied with the complete channel information available at all receivers and all senders, respectively. It was shown that single antenna/stream transmission maximizes the network capacity in the asymptotically high SIR regime. In [8], a closed-loop formula for the capacity of a MIMO link in an arbitrary network given the availability of the channel information of all interfering transmissions at the receivers was presented. Similarly, closed-loop expressions for the error probability of adaptive antenna arrays were obtained assuming optimal combining [7, 22] and minimum mean square error (MMSE) combining with and without successive interference cancellation [36]. Alternatively, [14–16, 32] and references therein investigated the transmission capacity of MIMO networks defined as the number of simultaneous transmission per unit area for different MIMO physical layer schemes assuming a single data stream/antenna per sender. These prior works consider advanced transceiver architectures. For instance, [14] and [16] consider interference cancellation techniques that fully and partially cancel the strongest interferers, respectively. Meanwhile, [15] assumes advanced transmission techniques such as transmit beamforming, transmit antenna selection and space time codes in conjunction with maximal ratio combining at the receiver. However, all of the aforementioned prior work assumes a certain amount of information about the channels of interfering flows to be available at either flows' endpoints which necessitates a synchronized system. Synchronization and channel information exchange have been experimentally shown to significantly deteriorate the overall network performance [12]. In contrast to [5, 7, 8, 14–16, 22, 32, 35, 36], we are the first to *experimentally* evaluate interfering synchronous and asynchronous MIMO flows without the availability of the channel information of interfering flows. Prior experimental MIMO research was concerned with the assessment of the performance of an individual MIMO link (e.g., see [21, 27]).

7 Conclusions

In this paper, we have proposed using the multi-antenna physical layer to increase the number of spatially-proximate transmissions instead of increasing the per-link rate. A sender uses a single antenna for transmission while a receiver uses all of its antennas to provide diversity gain. We have experimentally demonstrated that such a physical layer is robust to uncoordinated and asynchronous interfering transmissions. We have

presented the simple modifications required to the 802.11 protocol to enable multiple SIMO flows to concurrently share the medium. We have shown that such a multi-flow SIMO MAC alleviates the severe unfairness of legacy 802.11 MIMO MAC in multi-hop topologies. We have developed an analytical model to compute the optimal carrier at a given node density for random networks.

Appendix

A. Analytical Proof of SIMO Robustness to Unknown Interference

Here, we analytically prove SIMO robustness properties using outage analysis. Time is slotted and in each slot the Rayleigh channel matrices between different sender-receiver pairs are unchanged. Given our interference-limited network model, consider a tagged sender that transmits n_s independent data streams from n_s antennas each with rate r and power P . Due to the independence of the data streams transmitted by a $n_s \times N$ flow, the achievable flow rate can be calculated as

$$R_s = n_s r (1 - p_{out})^{n_s} \quad (\text{A1})$$

where, p_{out} is the outage probability per stream (or antenna). Without loss of generality, we consider a single interferer that uses n_i antennas. The maximal ratio combiner uses the channel gain of the tagged sender as the weights of the combiner [1, 10]. The received SINR of the k^{th} stream at the output of the maximal ratio combiner is given by

$$SINR = \frac{\tilde{P}_s \mathbf{h}_{k,s}^\dagger \mathbf{h}_{k,s}}{\sum_{l=1}^{n_i} \tilde{P}_i \frac{|\mathbf{h}_{k,s}^\dagger \mathbf{h}_{l,i}|^2}{\mathbf{h}_{k,s}^\dagger \mathbf{h}_{k,s}} + \sigma^2} \quad (\text{A2})$$

where \tilde{P}_s and \tilde{P}_i are the path-loss components of received signal power from the tagged and interfering senders per antenna, respectively, and \dagger is the complex conjugate transpose. The vector $\mathbf{h}_{k,s}$ and $\mathbf{h}_{l,i}$ represent the channel gain vectors of the k^{th} transmit antenna of the tagged sender s , and the l^{th} interfering antenna of the interferer i , respectively, and the receiver. We define the following terms to describe the output of the maximal ratio combiner: $\gamma = \mathbf{h}_{k,s}^\dagger \mathbf{h}_{k,s} = \sum_{m=1}^N |h_{km,s}|^2$ as the effective SIMO channel of the k^{th} transmit antenna at the output of the combiner, where $h_{km,s}$ is the channel fading coefficient between the k^{th} transmit antenna and the m^{th} receive antenna; and $\tilde{\gamma} = \sum_{l=1}^{n_i} \frac{|\mathbf{h}_{k,s}^\dagger \mathbf{h}_{l,i}|^2}{\mathbf{h}_{k,s}^\dagger \mathbf{h}_{k,s}}$ as the effective interference at the combiner output. Hence, (A2) can be rewritten as

$$SINR = \frac{SIR\gamma}{\tilde{\gamma} + \frac{\sigma^2}{\tilde{P}_i}} \quad (\text{A3})$$

where $SIR = \tilde{P}_s/\tilde{P}_i$ is the signal to interference ratio per antenna. Substituting in (18), the outage probability can be expressed as

$$p_{out} = Prob \left[\frac{\gamma}{\tilde{\gamma} + \frac{\sigma^2}{\tilde{P}_i}} < \frac{(2^r - 1)}{SIR} \right] \quad (\text{A4})$$

For Raleigh fading channel coefficients, $|h_{km,s}|^2$ and $|\mathbf{h}_{k,s}^\dagger \mathbf{h}_{l,i}|^2$ $\mathbf{h}_{k,s}^\dagger \mathbf{h}_{k,s}$ are exponentially distributed [1, 10]. The Chi-square (χ_m^2) distribution with m degrees of freedom nominally applies to the sum of m *i.i.d.* exponential random variables. Since the channel fading coefficients are *i.i.d.*, γ and $\tilde{\gamma}$ are Chi-square distributed with $2N$ and $2n_i$ degrees of freedom, respectively. Thus, the outage probability in (A4) is calculated as

$$p_{out} = \int_0^\infty f_{\tilde{\gamma}}(\tilde{\gamma}) \int_0^{A(\tilde{\gamma} + \frac{\sigma^2}{\tilde{P}_i})} f_{\gamma}(\gamma) d\gamma d\tilde{\gamma} \quad (\text{A5})$$

$$= 1 - \frac{e^{-\frac{A\sigma^2}{\tilde{P}_i}}}{\Gamma(n_i)} \sum_{s=0}^{N-1} \frac{A^s}{s!} \int_0^\infty \tilde{\gamma}^{n_i-1} \left(\tilde{\gamma} + \frac{\sigma^2}{\tilde{P}_i}\right)^s e^{-\tilde{\gamma}(1+A)} d\tilde{\gamma} \quad (\text{A6})$$

where $A = \frac{(2^r - 1)}{SIR}$. For interference-limited networks, the signal and interference powers are much higher than the noise power (i.e., $\tilde{P}_s \gg \sigma^2$ and $\tilde{P}_i \gg \sigma^2$), the intractable integral in (A6) is reduced to a tractable one that equals $(s + n_i - 1)! / (1 + A)^{s + n_i}$, and hence (A6) is equal to

$$p_{out} \cong 1 - \frac{1}{\Gamma(n_i)(1+A)^{n_i}} \sum_{s=0}^{N-1} \left(\frac{A}{1+A}\right)^s \frac{(s+n_i-1)!}{s!} \quad (\text{A7})$$

Thus, the outage probability, and hence, the achievable flow rate R_s is a function n_s , n_i , the SIR , and the stream rate r .

To illustrate the increase in the required SIR to obtain spatial multiplexing gain, we plot the achievable rate R_s normalized to the stream rate r for different number of transmit antennas. We consider two symmetric uncoordinated flows (i.e., $n_s = n_i$) with 4-antenna receivers. As depicted in Figure A1(a), SIMO robustness yields almost unity normalized flow rate even at low SIR . As the number of antennas per flow increases, the SIR required to obtain the promised gain increases, as experimentally demonstrated in Section 3.2. This trend is independent of the stream rate r . As r increases, the SIR required for higher spatial multiplexing degrees further increases.

Similar analysis can be performed considering L SIMO interferers each with power $\frac{P_{tot}}{L}$. We reevaluate the outage probability in such a multi-interferer scenario. Figure A1(b) depicts the achievable SIMO rate for different values of L with the total power fixed. Similar increase in the SIMO flow rate given more interferers was experimentally shown in Section 3.2. It is worth mentioning that for a given P_{tot} , the variance of the cumulative interference term in SINR is inversely proportional to L .

B. Characteristic Function of Received Interference

Conditioning on a certain channel instance $\gamma_k = \gamma$, the path-loss component of the received power per interferer $\tilde{P} = P_0 \left(\frac{d_0}{d}\right)^\alpha$ has the following distribution

$$f_{\tilde{P}}(x) = \frac{2P_0^{2/\alpha} d_0^2}{\alpha(D^2 - \varepsilon^2)x^{(\alpha+2)/\alpha}} \quad (\text{B1})$$

defined in the interval $[(\frac{d_0}{D})^\alpha P_0, (\frac{d_0}{\varepsilon})^\alpha P_0]$.

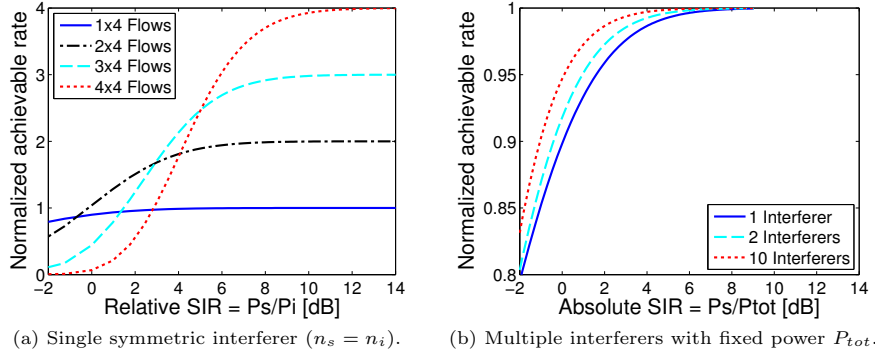


Fig. A1 Theoretical validation of SIMO properties.

By definition, the characteristic function of the random variable $P_{k|\gamma}$ is given by

$$\phi_{P_{k|\gamma}}(\omega) = \mathbb{E}[e^{(j\omega P_k)} | \gamma_k = \gamma] \quad (B2)$$

$$= \int_{(\frac{d_0}{D})^\alpha P_0}^{(\frac{d_0}{\epsilon})^\alpha P_0} e^{(j\omega x \gamma)} f_{\bar{P}}(x) dx \quad (B3)$$

$$= \frac{2P_0^{2/\alpha} d_0^2}{\alpha(D^2 - \epsilon^2)} \int_{(\frac{d_0}{D})^\alpha P_0}^{(\frac{d_0}{\epsilon})^\alpha P_0} \frac{e^{(j\omega x \gamma)}}{x^{(\alpha+2)/\alpha}} dx \quad (B4)$$

We use the distribution of the effective channel fading process given by (3) to remove the conditioning in (B2) as follows,

$$\phi_{P_k}(\omega) = \int_0^\infty \phi_{k|\gamma}(\omega) f_\gamma(\gamma) d\gamma \quad (B5)$$

$$= \frac{2P_0^{2/\alpha} d_0^2}{\alpha(R^2 - \epsilon^2)} \int_0^\infty \int_{(\frac{d_0}{D})^\alpha P_0}^{(\frac{d_0}{\epsilon})^\alpha P_0} \frac{e^{(j\omega x \gamma)} \gamma^{N-1} e^{-\gamma}}{\Gamma(N) x^{(\alpha+2)/\alpha}} dx d\gamma \quad (B6)$$

$$= \frac{2P_0^{2/\alpha} d_0^2}{\alpha(D^2 - \epsilon^2)} \int_{(\frac{d_0}{D})^\alpha P_0}^{(\frac{d_0}{\epsilon})^\alpha P_0} \frac{1}{x^{(\alpha+2)/\alpha} (1 - j\omega x)^N} dx \quad (B7)$$

which is what is given by (9).

References

1. Aalo, V., Chayawan, G.: Outage probability of cellular radio systems using maximal ratio combining in rayleigh fading channel with multiple interferers. *Electronics Letters* **36**(15), 1314 – 1315 (2000)
2. Adya, A., Bahl, P., Padhye, J., Wolman, A., Zhou, L.: A multi-radio unification protocol for IEEE 802.11 wireless networks. In: *Proceedings of BroadNets* (2004)
3. Alamouti, S.M.: A simple transmit diversity technique for wireless communications. *IEEE Journal on Selected Areas in Communications* **16**(8), 1451 –1458 (1998)

4. Bhatia, R., Li, L.: Throughput optimization of wireless mesh networks with MIMO links. In: Proceedings of IEEE INFOCOM '07. Anchorage, Alaska (2007)
5. Blum, R.: MIMO capacity with interference. *IEEE Journal on Selected Areas in Communications* **21**(5), 793–801 (2003)
6. Casari, P., Levorato, M., Zorzi, M.: DSMA: an access method for MIMO ad hoc networks based on distributed scheduling. In: Proceedings of ACM IWCMC. Vancouver, Canada (2006)
7. Chiani, M., Win, M., Zanella, A.: On optimum combining of M-PSK signals with unequal-power interferers and noise. *IEEE Transactions on Communications* **53**(1), 44 – 47 (2005)
8. Chiani, M., Win, M.Z., Shin, H.: MIMO network: the effects of interference. *IEEE Transaction of Information Theory* **56**(1), 336 – 349 (2010)
9. Choudhury, R.R., Yang, X., Vaidya, N.H., Ramanathan, R.: Using directional antennas for medium access control in ad hoc networks. In: Proceedings of ACM Mobicom'02 (2002)
10. Cui, J., Sheikh, A.: Outage probability of cellular radio systems using maximal ratio combining in the presence of multiple interferers. *IEEE Transactions on Communications* **47**(8), 1121 – 1124 (1999)
11. Garetto, M., Saloniadis, T., Knightly, E.: Modeling per-flow throughput and capturing starvation in CSMA multi-hop wireless networks. *IEEE/ACM Transactions on Networking* **16**(4), 864–877 (2008)
12. Gaur, S., Jiang, J.S., Ingram, M., Demirkol, M.: Interfering MIMO links with stream control and optimal antenna selection. In: Proceedings of IEEE Globecom'04. Dallas, TX (2004)
13. Gollakota, S., Katabi, D.: Zigzag decoding: Combating hidden terminals in wireless networks. In: Proceedings of the ACM SIGCOMM 2008. Seattle, WA (2008)
14. Huang, K., Andrews, J.G., Jr., R.W.H., Guo, D., Berry, R.: Spatial interference cancellation for multi-antenna mobile ad hoc networks. *IEEE Transactions on Information Theory* (submitted). (arXiv:0807.1773v2)
15. Hunter, A.M., Andrews, J.G., Weber, S.P.: Transmission capacity of ad hoc networks with spatial diversity. *IEEE Transactions on Wireless Communications* **7**(12), 5058 – 5071 (2008)
16. Jindal, N., Andrews, J.G., Weber, S.: Multi-antenna communication in ad hoc networks: Achieving MIMO gains with SIMO transmission. *IEEE Transactions on Communications* **59**(2), 529 –540 (2011)
17. Kelly, F., Maulloo, A., Tan, D.: The rate control for communication networks: shadow prices, proportional fairness and stability. *Journal of the Operational Research Society* **40**9, 237–252 (1998)
18. Khattab, A.: An experimental case for SIMO random access in multi-antenna multi-hop wireless networks. In: Proceedings of the IEEE INFOCOM 2010. San Diego, CA (2010)
19. Khattab, A., Camp, J., Hunter, C., Murphy, P., Sabharwal, A., Knightly, E.: WARP: A flexible platform for clean-slate wireless medium access protocol design. *SIGMOBILE Mob. Comput. Commun. Rev.* pp. 56–58 (2008)
20. Khattab, A., Sabharwal, A., Knightly, E.W.: Asynchronous randomized allocation multi-antenna medium access in multi-hop networks. In: Proceedings of IEEE ICCCN 2008. St. Thomas, US (2008)
21. Kim *et al*, W.: An experimental evaluation of rate adaptation for multi-antenna systems. In: Proceedings of the IEEE INFOCOM 2009. Rio de Janeiro, Brazil

- (2009)
22. McKay, M., Zanella, A., Collings, I., Chiani, M.: Error probability and SINR analysis of optimum combining in rician fading. *IEEE Transactions on Communications* **57**(3), 676–687 (2009)
 23. Papoulis, A.: *The Fourier Integral and its Applications*. New York: McGraw-Hill (1962)
 24. Park, M., Heath, R.J., Nettles, S.: Improving throughput and fairness for MIMO ad hoc networks using antenna selection diversity. In: *Proceedings of IEEE Globecom'04* (2004)
 25. Radunovic, B., Gunawardena, D., Proutiere, A., Singh, N., Balan, V., Key, P.: Efficiency and fairness in distributed wireless networks through self-interference cancellation and scheduling. Tech. Rep. MSR-TR-2009-27, Microsoft Research, Cambridge, UK (2009)
 26. Santhapuri, N., Manweiler, J., Sen, S., Choudhury, R.R., Nelakuditi, S., Munagala, K.: Message in message (MIM): A case for reordering transmissions in wireless networks. In: *Proceedings of ACM HotNets*. Alberta, Canada (2008)
 27. Shrivastava, V., Rayanchu, S., Yoon, J., Banerjee, S.: 802.11n under the microscope. In: *Proceedings of the ACM/USENIX Internet Measurement Conference (IMC '08)*. Vouliagmeni, Greece (2008)
 28. So, J., Vaidya, N.H.: Multi-channel mac for ad hoc networks: handling multi-channel hidden terminals using a single transceiver. In: *Proceedings of ACM MobiHoc'04*. Tokyo, Japan (2004)
 29. Sundaresan, K., Sivakumar, R., Ingram, M., Chang, T.Y.: A fair medium access control protocol for ad-hoc networks with MIMO links. In: *Proceedings of IEEE INFOCOM 2004*. Hong Kong (2004)
 30. Telatar, I.E.: Capacity of multi-antenna gaussian channels. *European Transactions on Telecommunications* **10**(6), 585–595 (1999)
 31. Tse, D., Viswanath, P.: *Fundamentals of Wireless Communication*. Cambridge University Press (2005)
 32. Weber, S., Andrews, J., Jindal, N.: An overview of the transmission capacity of wireless networks. *Communications, IEEE Transactions on* **58**(12), 3593–3604 (2010)
 33. Wolniansky, P.W., Foschini, G.J., Golden, G.D., Valenzuela, R.A.: V-BLAST: An architecture for realizing very high data rates over the rich-scattering wireless channel. In: *Proceedings of IEEE ISSSE 98*. Pisa, Italy (1998)
 34. Yao, Y.D., Sheikh, A.: Investigations into cochannel interference in microcellular mobile radio systems. *IEEE Transactions on Vehicular Technology* **41**(2), 114–123 (1992)
 35. Ye, S., Blum, R.: Optimized signaling for MIMO interference systems with feedback. *IEEE Transactions on Signal Processing* **51**, 2839–2848 (2003)
 36. Zanella, A., Chiani, M., Win, M.: MMSE reception and successive interference cancellation for MIMO systems with high spectral efficiency. *IEEE Transactions on Wireless Communications* **4**(3), 1244–1253 (2005)